Supplementary Material

Regulation of Calcium-Calcineurin Signaling by miR-30s in Podocytes

Junnan Wu, Chunxia Zheng, Xiao Wang, Shifeng Yun, Yue Zhao, Lin Liu, Yuqiu Lu, Yuting Ye, Xiaodong Zhu, Changming Zhang, Shaolin Shi, and Zhihong Liu
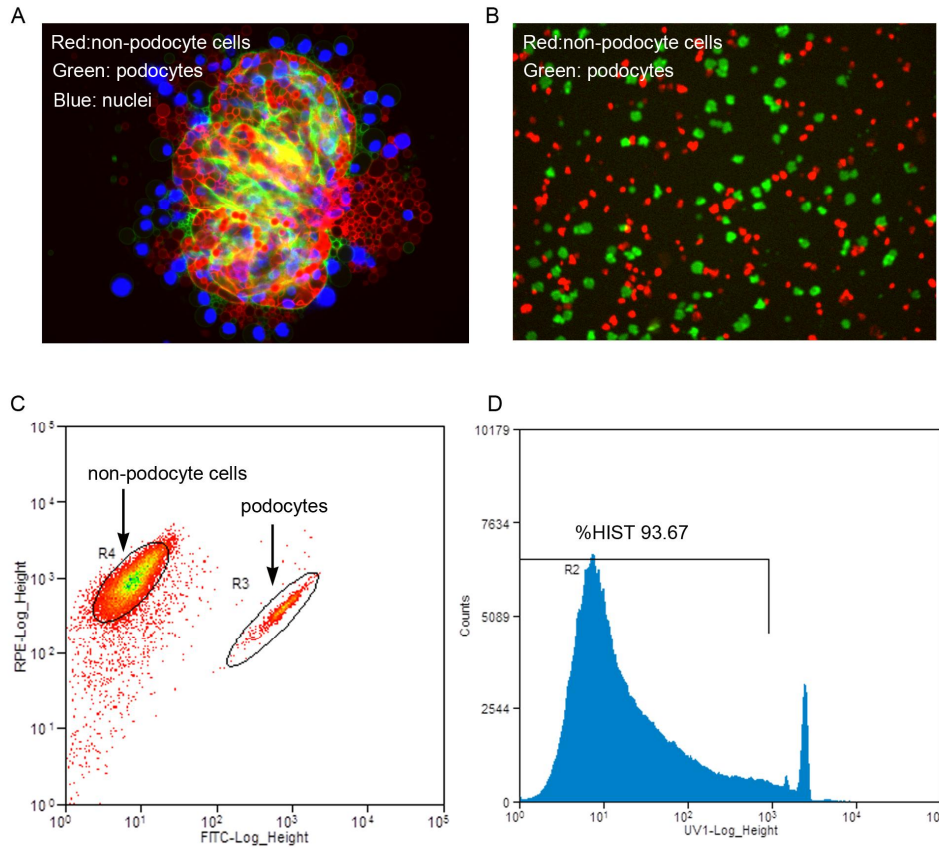
Supplemental Figure S1. Isolation of podocytes from mice. **A**. Fluorescence image of a glomerulus from a double-transgenic mouse obtained by crossing Gt(ROSA)26Sor$^{tm4(ACTB-tdTomato,-eGFP)Luo}$ transgene with NPHS2-Cre transgene. (original magnification, ×40). **B**. Fluorescence image of a single cell suspension after collagenase digestion of the glomeruli. (original magnification, ×10). **C**. Flow cytometric analysis of dissociated glomerular cells. **D**. The proportion of viable cells in the sample.
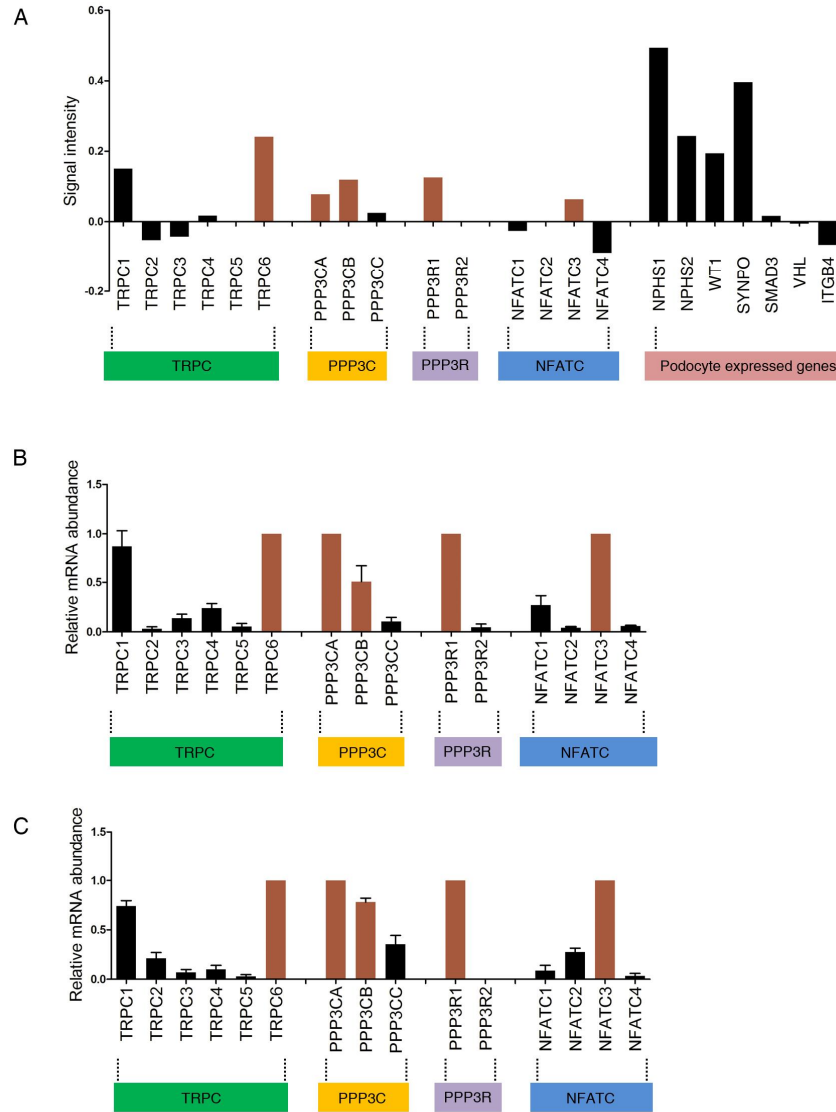
Supplemental Figure S2. TRPC6, PPP3CA, PPP3CB, PPP3R1 and NFATC3 mRNAs are expressed at high levels in human glomeruli. **A**. Signal intensities of the genes as indicated by a microarray (1). **B**. qPCR analysis of the indicated genes in human glomeruli (n=5), confirming the results in "A". **C**. qPCR analysis of these genes in immortalized human podocytes, showing that these cells retain the expression pattern shown in "B". The data are presented as the mean±SD of three independent experiments.
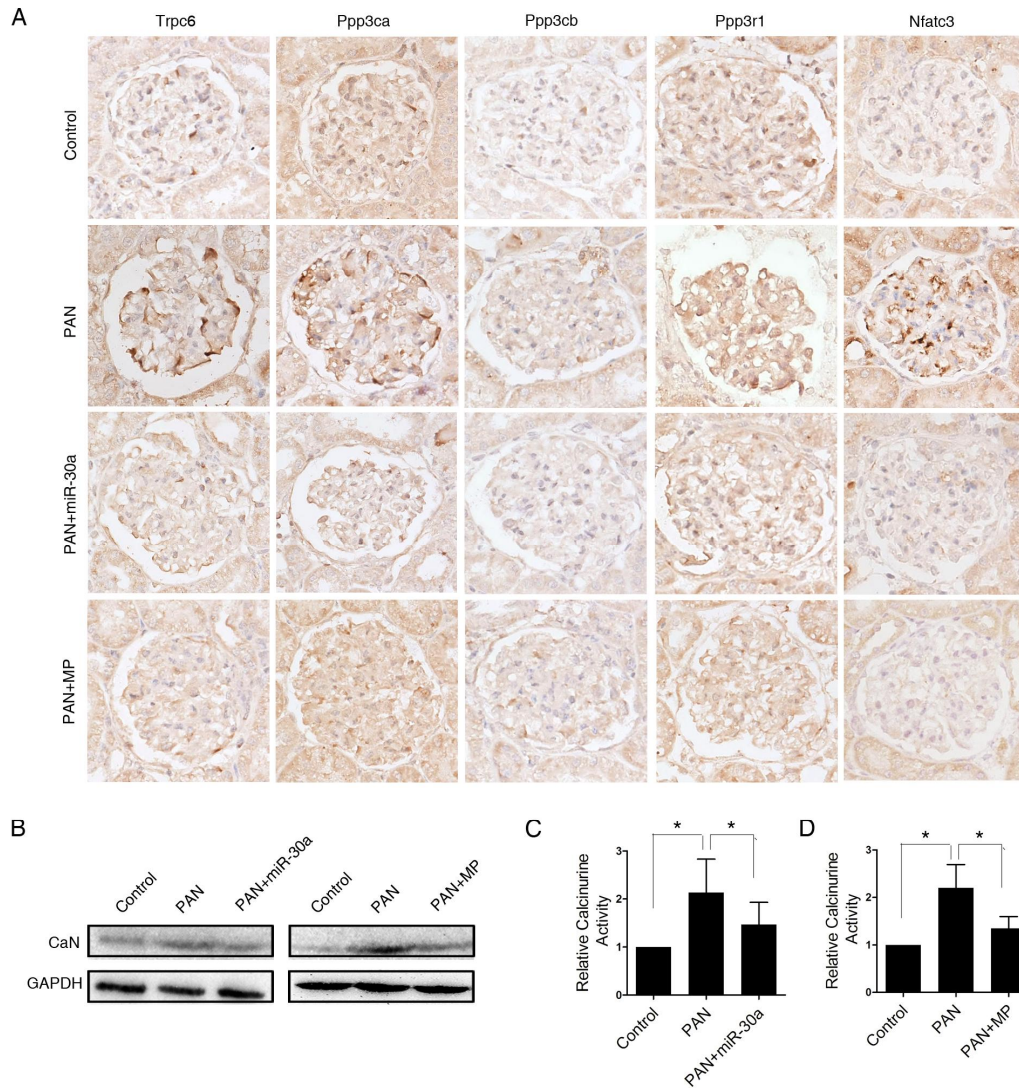
Supplemental Figure S3. Changes in the protein expression of Trpc6, Ppp3ca, Ppp3cb, Ppp3r1 or Nfatc3 in the podocytes of rats treated with PAN in the presence or absence of exogenous miR-30a or glucocorticoids. **A**. IHC of these proteins in the kidneys of rats treated as indicated (original magnification, ×40). miR-30a: *in vivo* delivery of the miR-30a expression plasmid preceding PAN treatment; MP: methylprednisolone. Representative images from 6 rats in each group are shown. **B**. Immunoblotting using an antibody against both the Ppp3ca and Ppp3cb proteins (CaN) in the glomeruli of PAN-treated rats confirmed the IHC results. Parallel gels were run for CaN and GAPDH, respectively. Representative blots from 3 independent experiments are shown. **C-D**. Relative calcineurin phosphatase activities in the glomeruli of PAN-treated rats that were or were not subjected to miR-30a delivery *in vivo* (C) or MP treatment (D) (n=8); Statistical analysis was performed with one-way ANOVA. *P<0.05.
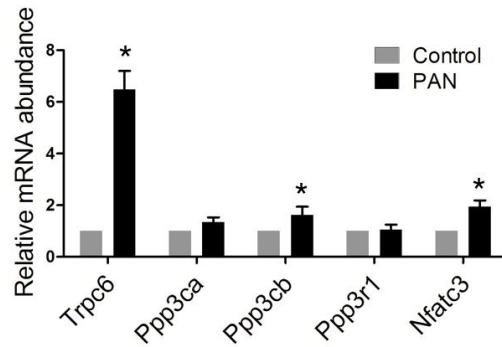
Supplemental Figure S4. qPCR analysis of the 5 indicated genes in the glomeruli of control and PAN-treated rats (n=5 for each group). Two-tailed Student's t-test, *P<0.05.
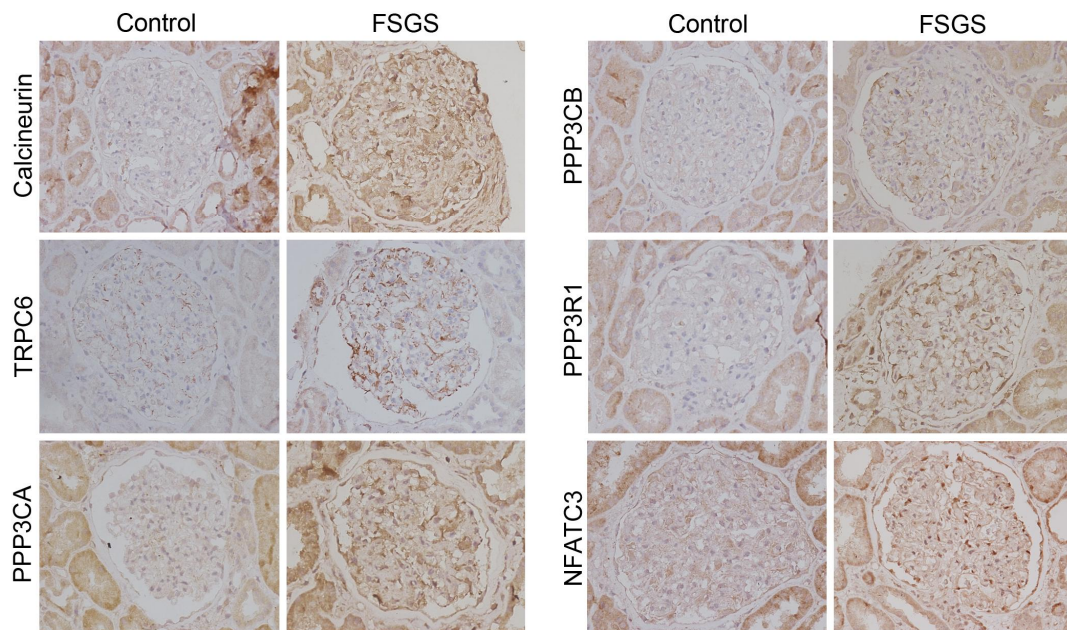
Supplemental Figure S5. IHC staining demonstrates that the levels of TRPC6, PPP3CA, PPP3CB, PPP3R1 and NFATC3 proteins were low in the glomeruli of controls but significantly upregulated in the FSGS patients (original magnification, ×40). Representative images from 4 subjects in each group are shown.
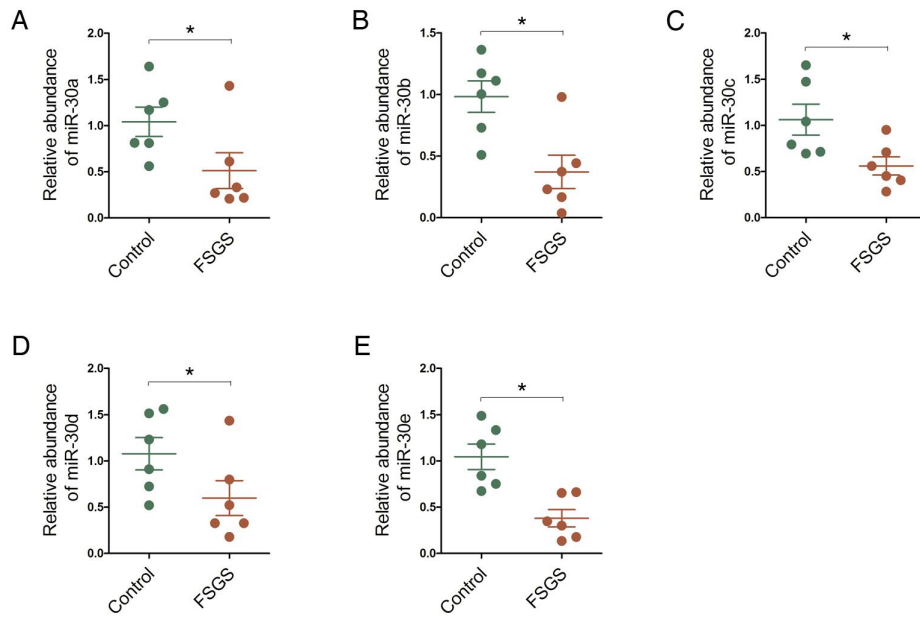
Supplemental Figure S6. miR-30s were downregulated in the glomeruli of FSGS patients compared with the controls (n = 6 in each group). Two-tailed Student's t-test, *P<0.05.
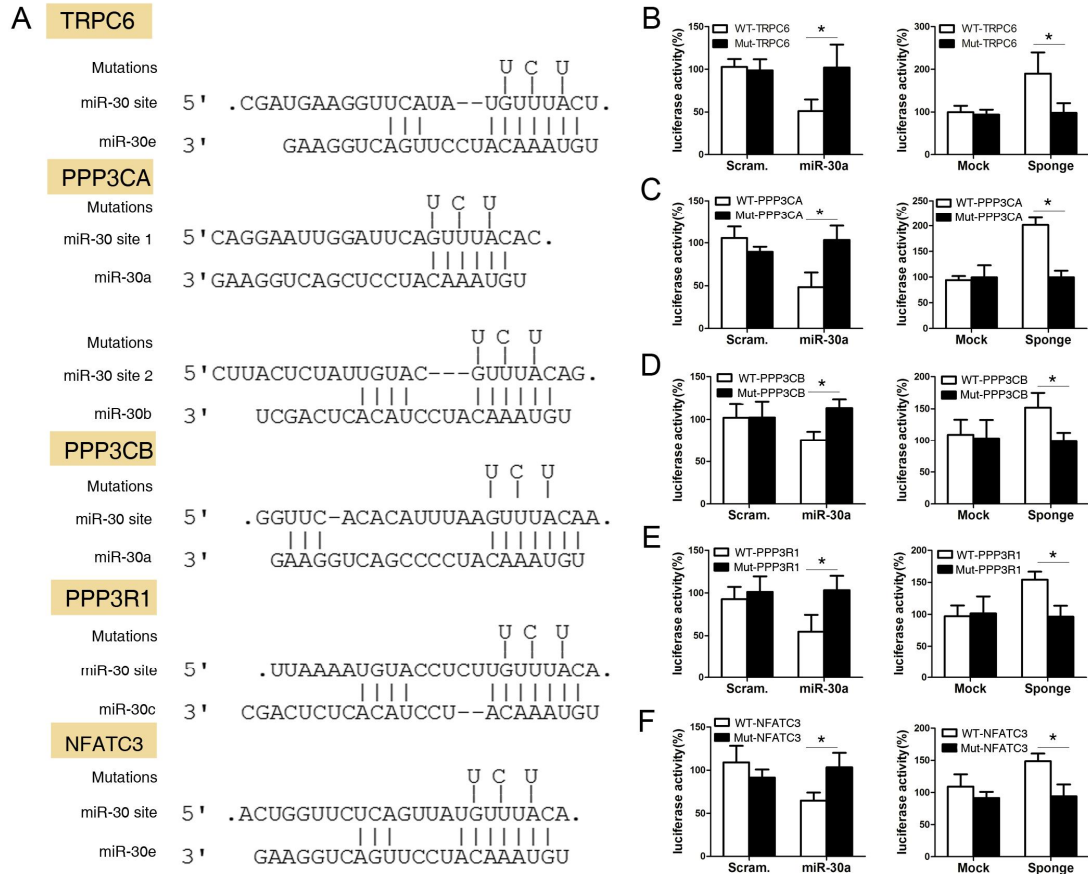
Supplemental Figure S7. Luciferase reporter assays to determine whether TRPC6, PPP3CA, PPP3CB, PPP3R1, or NFATC3 are miR-30 targets. **A**. Predicted miR-30-targeted sites in the 3'-UTRs of TRPC6, PPP3CA, PPP3CB, PPP3R1, and NFATC3. Mutations of three nucleotides as indicated were made for each mutant reporter construct. **B-F**. The effects of miR-30a overexpression or miR-30 knockdown using the miR-30 sponge on luciferase reporter expression. WT: wild type 3' UTR sequence; Mut: mutant 3' UTR sequence. All experiments were performed in triplicate, and the data are expressed as the mean±SD. Two-tailed Student's t-test, *P<0.05.
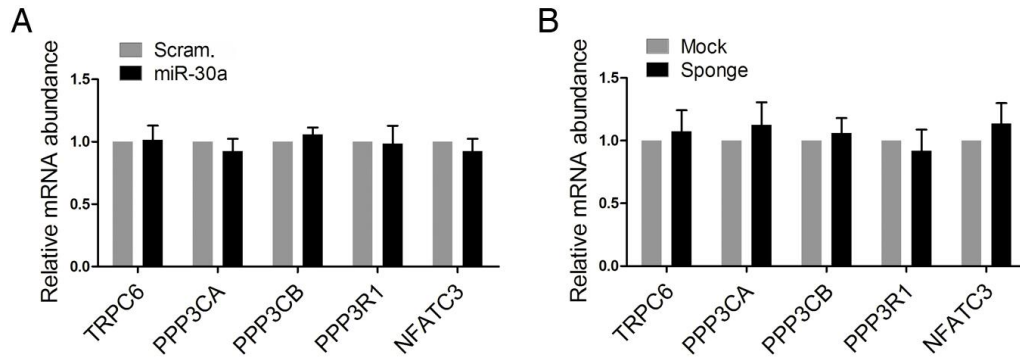
Supplemental Figure S8. Neither miR-30a overexpression (**A**) nor miR-30 sponge transfection (**B**) altered the mRNA levels of TRPC6, PPP3CA, PPP3CB, PPP3R1 and NFATC3 in human cultured podocytes. The data are presented as the mean±SD of three independent experiments.
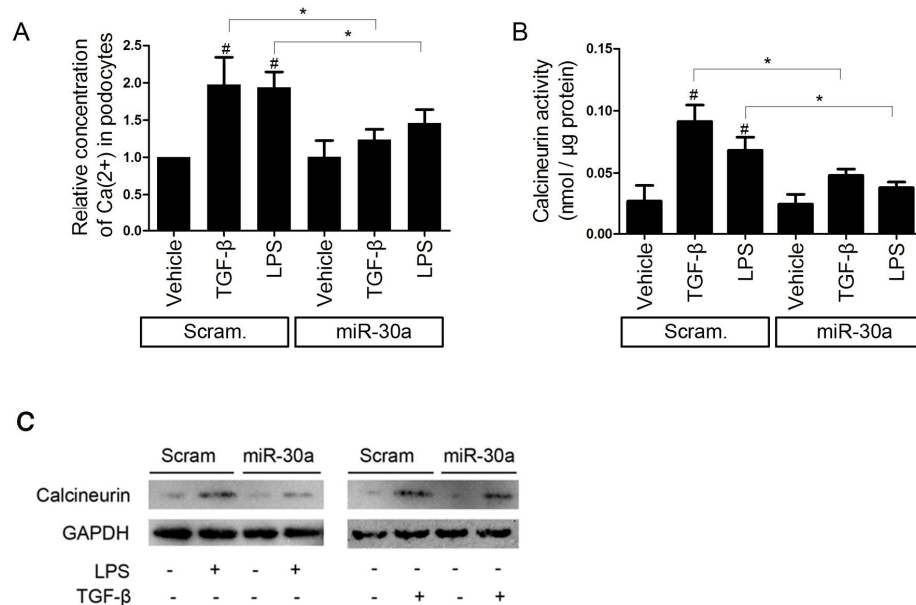
Supplemental Figure S9. TGF-β and LPS induce calcium-calcineurin signaling in cultured human podocytes. **A-B**. miR-30a overexpression alleviated TGF-β- or LPS-induced intracellular Ca^{2+} accumulation (A) and calcineurin phosphatase activity in the podocytes (B). All experiments were performed in triplicate, and the data are expressed as the mean±SD; two-way ANOVA, #P<0.05 (versus the vehicle-treated control); *P<0.05. **C**. Representative immunoblots showing that TGF-β or LPS upregulates calcineurin protein expression and that this effect was ameliorated by miR-30a overexpression. Parallel gels were run for calcineurin and GAPDH, respectively. Representative blots from 3 independent experiments are shown.
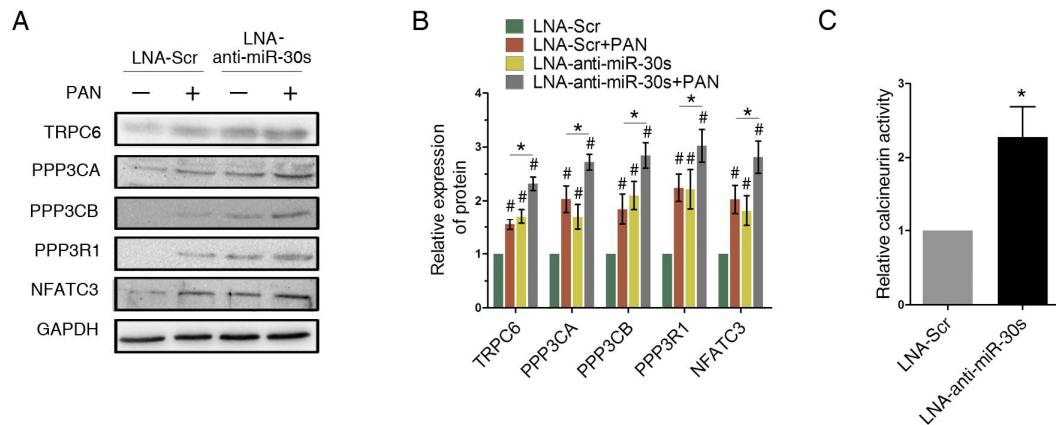
Supplemental Figure S10. LNA-Anti-miR-30s increased the expressions of TRPC6, PPP3CA, PPP3CB, PPP3R1 and NFATC3 in the cultured podocytes. **A**. Immunoblotting showing the miR-30 inhibitor increased the 5 proteins in the absence or presence of PAN. Parallel gels were run for the proteins indicated and GAPDH, respectively. **B**. Quantifications of "A" (n=3); One-way ANOVA,*P<0.05, #P<0.05. **C**. Transfection of the inhibitor increased calcineurin activity in the cells (n=3). Two-tailed Student's t-test, * P<0.05.
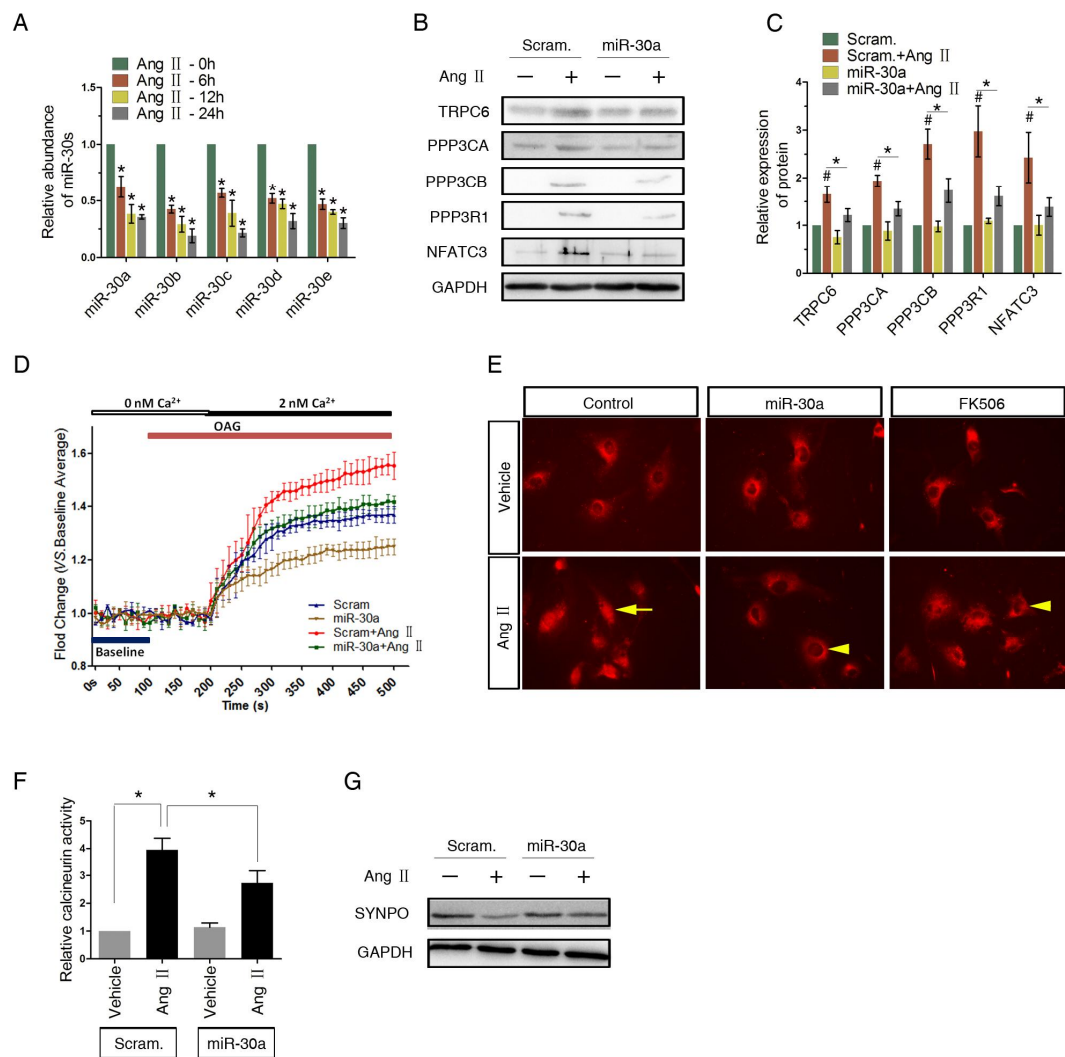
Supplemental Figure S11. miR-30s mediate Ang II-induced activation of calcium-calcineurin signaling. **A**. qPCR analysis showing that Ang II downregulated all miR-30 family members in podocytes (n=4). **B-C**. Ang II upregulated the protein expression of TRPC6, PPP3CA, PPP3CB, PPP3R1 and NFATC3, but these effects were attenuated by exogenous miR-30a. Quantification of the results from three independent experiments was performed. Parallel gels were run for the proteins indicated and GAPDH, respectively. **D**. Ang II induced calcium influx, which was attenuated by exogenous miR-30a (n=15-20 cells). **E**. Immunofluorescence staining demonstrates that Ang II induced NFATC3 nuclear translocation (arrow), and exogenous miR-30a and FK506 could inhibit NFATC3 nuclear translocation (arrowheads) (original magnification, ×20). Representative images from 3 independent experiments are shown. **F**. Calcineurin phosphatase assay shows that Ang II increased calcineurin activity and exogenous expression of miR-30a could partially prevent it. **G**. Immunoblotting showing the downregulation of synaptopodin by Ang II, which was prevented by exogenous miR-30a transfection. Parallel gels
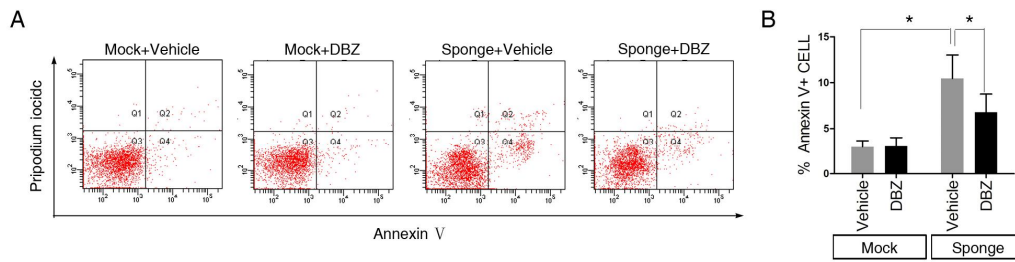
Supplemental Figure S12. The Notch signaling inhibitor DBZ partially protects the cultured podocytes from miR-30 sponge-induced apoptosis. **A**. Flow cytometry analysis of Annexin V-stained cultured human podocytes treated with the miR-30 sponge in the presence or absence of DBZ. **B**. Quantification of the results from triplicate experiments. The data are expressed as the mean±SD; two-way ANOVA, *P<0.05.
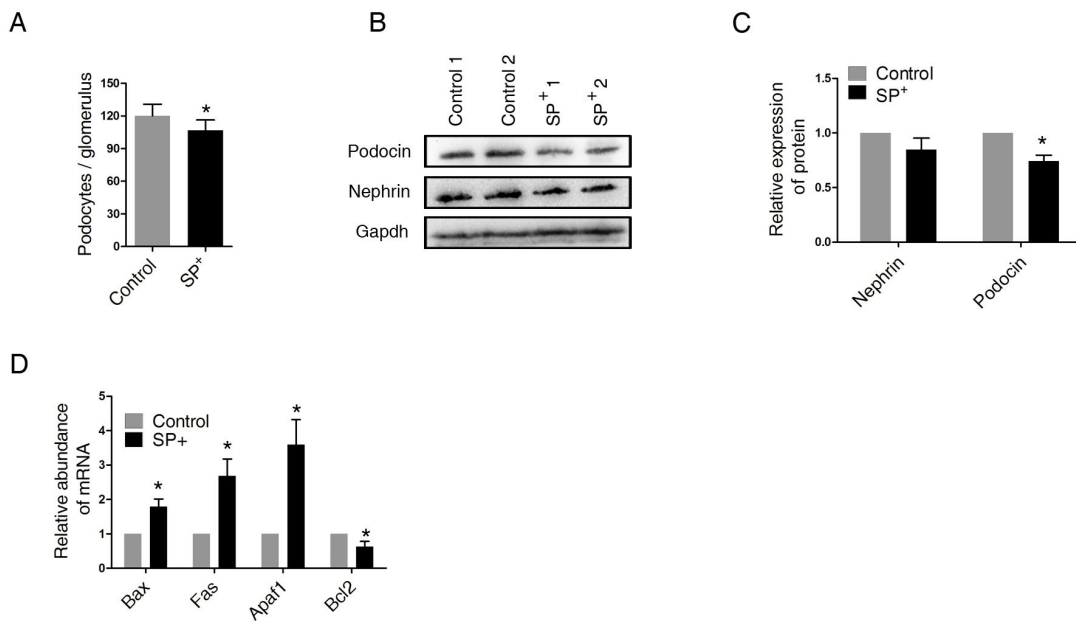
Supplemental Figure S13. Characterization of the SP+ mice. **A**. Podocyte counting for the glomeruli revealed an 11.8% reduction in the podocyte number in SP$^+$ mice (n=8). Two-tailed Student's t-test, *P<0.05. **B-C**. Immunoblotting with the glomeruli revealed a reduction of podocin or nephrin in the SP+ mice (P=0.063) (n=4). Two-tailed Student's t-test, *P<0.05. **D**. The proapoptotic markers Bax, Fas and Apaf1 were upregulated, whereas anti-apoptotic Bcl2 was downregulated in the glomeruli of the SP+ mice (n=6). Two-tailed Student's t-test, *P<0.05.
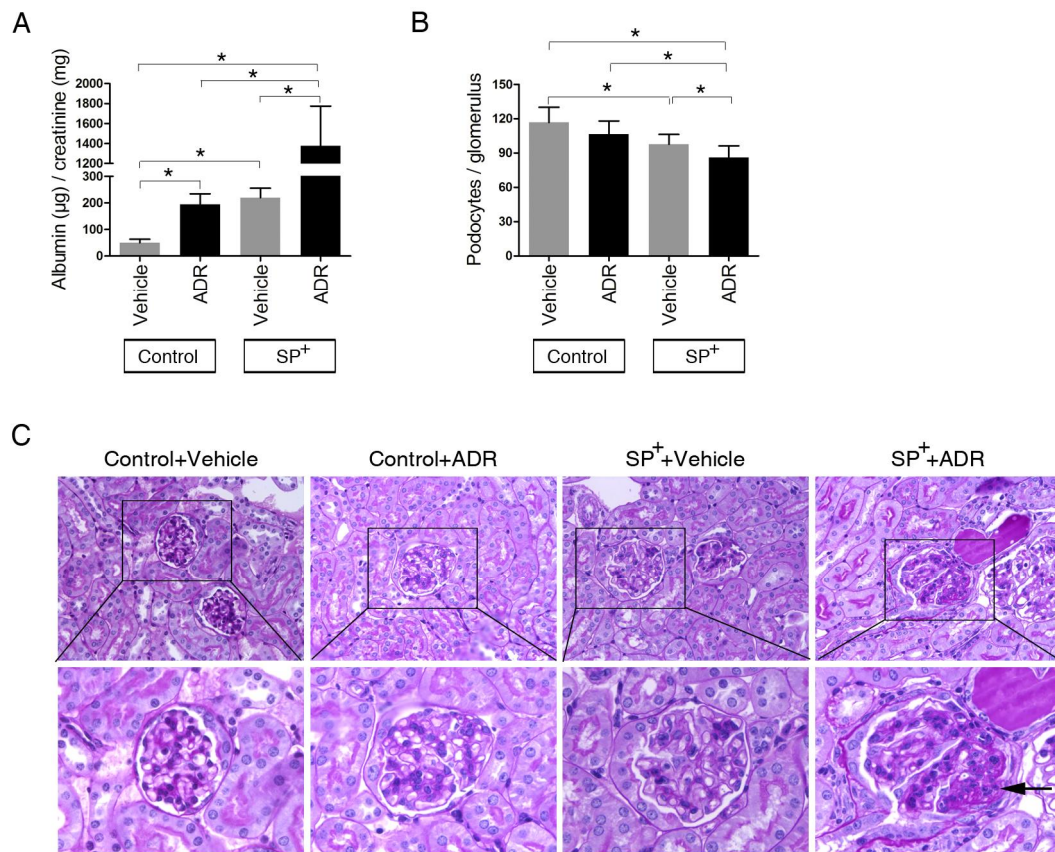
Supplemental Figure S14. miR-30 sponge transgenic mice exhibited increased sensitivity to ADR compared to control mice. Control and SP[+] mice were treated with ADR at 10 weeks of age. Three weeks following ADR injection, urine samples were collected and the mice were sacrificed for kidney histology. **A**. albuminuria was assessed for each group indicated (n=6); two-way ANOVA, *$P<0.05$. **B**. podocyte counting of each group; two-way ANOVA, *$P<0.05$. **C**. PAS was used to evaluate glomerular changes (top panel: original magnification, ×40; bottom panel: original magnification, ×100). Representative images from 6 mice in each group are shown. The arrow points to the sclerotic area of a glomerulus.
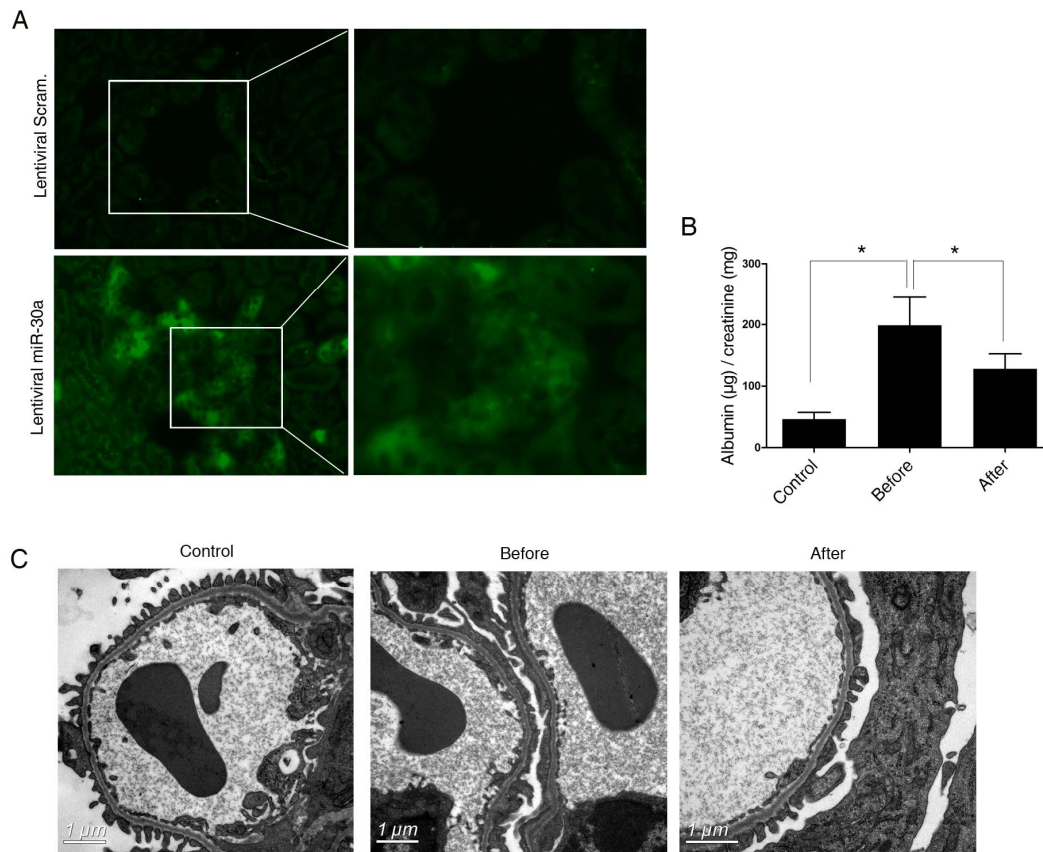
Supplemental Figure S15. The specificity of the miR-30 sponge transgene is demonstrated via the lentiviral expression of miR-30a in the SP$^+$ mouse podocytes. **A**. Fluorescence microscopy showing eGFP expression, thus indicating miR-30a expression, in the glomeruli of mice at 3 days after miR-30a lentivirus injection (left panel: original magnification, ×40; right panel: original magnification, ×100). **B**. Proteinuria in the SP+ mice was greatly reduced at 3 days after miR-30a lentivirus injection (n=8 in each group); one-way ANOVA, *P<0.05. Control: normal control mice not subjected to lentivirus injection; Before: SP$^+$ mice before lentivirus injection; After: the same SP+ mice at 3 days after lentivirus injection. **C**. Representative EM images of the glomeruli of the mice shown in "B", demonstrating the improvement of foot process effacement after lentivirus injection. Scale bars: 1μm. Representative images from 8 mice in each group are shown.
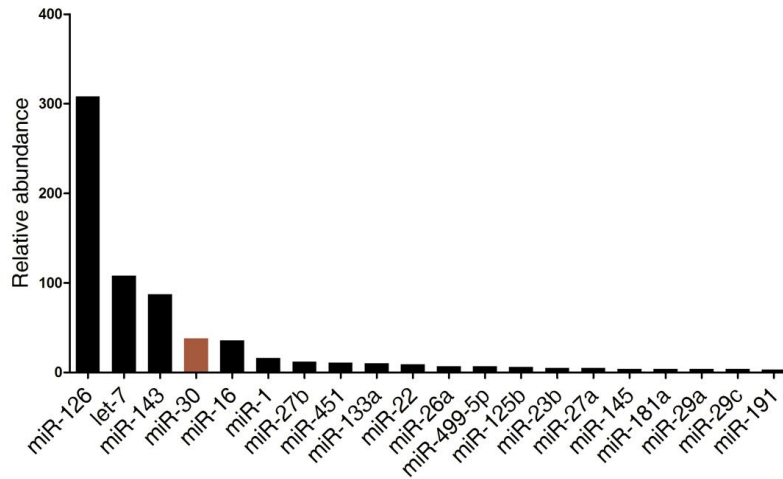
Supplemental Figure S16. Relative abundance of the top 20 miRNAs in the human heart based on smiRNAdb (http://www.mirz.unibas.ch).
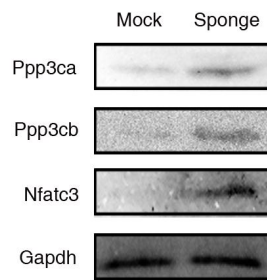
Supplemental Figure S17. Representative immunoblots showing that the miR-30 sponge increases Ppp3ca, Ppp3cb and Nfatc3 protein expression in cultured cardiomyocytes. Parallel gels were run for the proteins indicated and Gapdh. Representative blots from 3 independent experiments are shown.
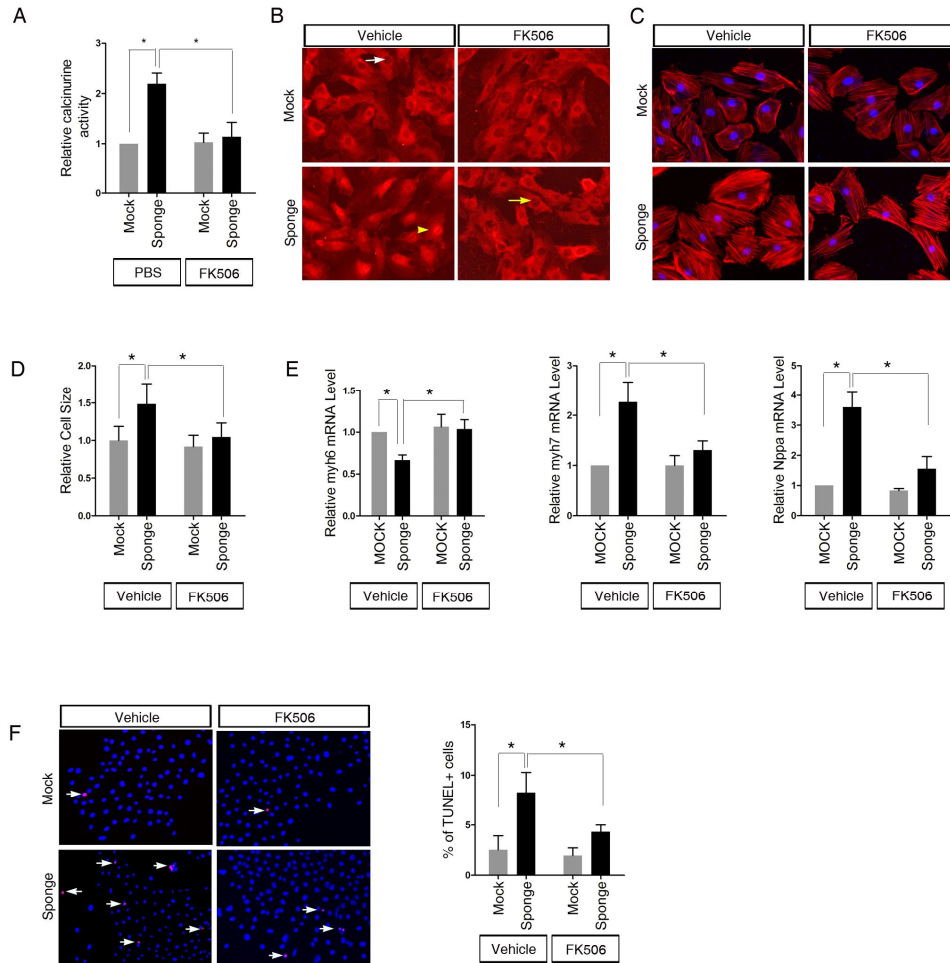
Supplemental Figure S18. miR-30 knockdown induces calcium-calcineurin signaling in cultured cardiomyocytes. **A**. A calcineurin phosphatase assay with the cells transfected with a miR-30 sponge revealed an increase in calcineurin phosphatase activity in the miR-30-silenced cells. This effect was prevented by FK506 treatment (n=4) ; two-way ANOVA, *P<0.05. **B**. IF staining for Nfatc3 in the cells transfected with a miR-30 sponge. The nuclear accumulation of Nfatc3 was clearly observed in the cells, and FK506 prevented the translocation of Nfatc3 (original magnification, ×20). Representative images from 3 independent experiments are shown. **C**. Phalloidin staining of the cardiomyocytes treated with a miR-30 sponge in the presence or absence of FK506 (original magnification, ×20). **D**. Calculation of the cell size based on phalloidin staining in "C", which revealed that the miR-30 sponge increased the cell size but that this effect was prevented by FK506 (n=20 cells). **E**. qPCR analysis of the gene expression of the hypertrophy markers Myh7, Nppa, and Myh6 in cardiomyocytes. The data are presented as the mean±SD of three experiments; two-way ANOVA, *P<0.05. **F**. The TUNEL assay revealed the increased apoptosis of the cells transfected with the miR-30 sponge (white arrows). This effect was mitigated by FK506 (original magnification, ×10). The percentages of TUNEL-positive cells per high-power field (HPF) (n=10) were calculated. The results are shown on the right; two-way ANOVA, *P<0.05.
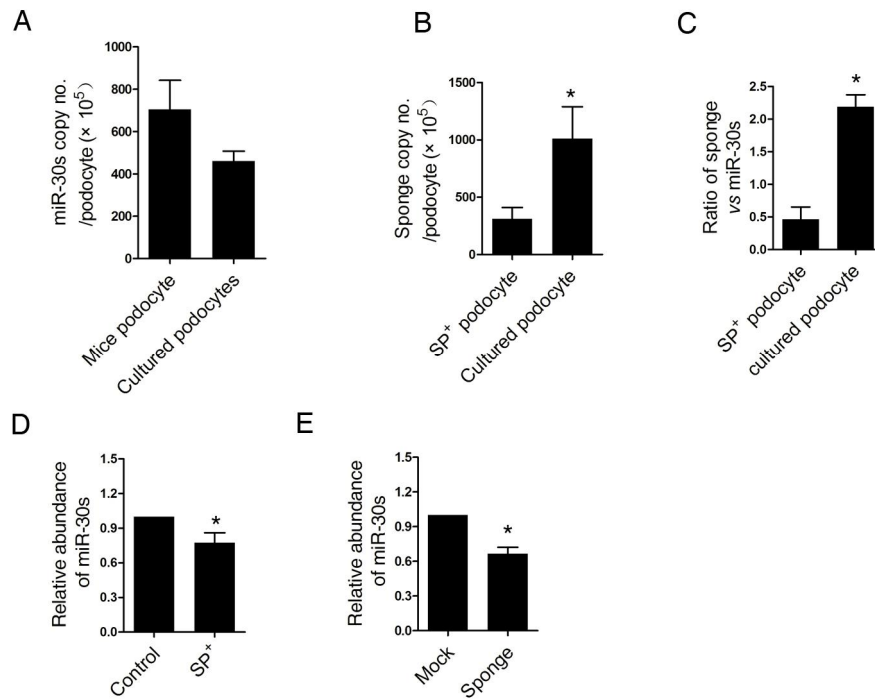
Supplemental Figure S19. qPCR quantification of miR-30s and miR-30 sponge in the podocytes of SP$^+$ mice and cultured podocytes transfected with sponge. **A**. The comparable miR-30 copy numbers (per cell) in the podocytes of a mouse and in cultured podocytes (n=3). **B**. The copy numbers of sponge in the podocytes of the SP$^+$ mice and the sponge-transfected cultured podocytes (n=3). **C**. The ratios of copy numbers of sponge versus miR-30s in the podocytes of the SP$^+$ mice and in the cultured podocytes transfected with sponge (n=3). **D-E**. Relative miR-30 levels in the podocytes of control mice versus SP$^+$ (D) and in the cultured podocytes that were mock transfected versus podocytes that were transfected with the sponge (n=3) (E), showing that the sponge reduced the level of miR-30s in both cases (n=3). Statistical analysis performed with two-tailed Student's t-test, *P<0.05.

Supplemental Table S1. Top 10 pathways predicted to be targeted by miR-30s

Ingenuity Canonical Pathways[1]	-log(p-value)	Ratio
Axonal Guidance Signaling [2]	7.78E00	1.32E-01
Cardiac Hypertrophy Signaling [2]	4.14E00	1.27E-01
IGF-1 Signaling	4.1E00	1.68E-01
B Cell Receptor Signaling [2]	3.7E00	1.41E-01
Calcium Signaling	3.3E00	1.16E-01
PKCθ Signaling in T Lymphocytes [2]	3.26E00	1.27E-01
PI3K Signaling in B Lymphocytes [2]	3.24E00	1.36E-01
T Cell Receptor Signaling [2]	3.22E00	1.47E-01
Reelin Signaling in Neurons	3.2E00	1.71E-01
Amyotrophic Lateral Sclerosis Signaling	3.12E00	1.34E-01

Notes:

1. The 1357 genes that are predicte by TargetScan to be targets of the miR-30 family were analyzed via IPA.
2. These pathways significantly overlap with Ca^{2+} signaling because they share many components; therefore, their components are essentially Ca^{2+} signaling-related factors.

Supplemental Table S2. The predicted miR-30 target genes in the calcium-calcineurin pathway

Calcium channel components:

   GRIN2A, TRDN, GRIA2, ATP2a2, ATP2b1, ATP2b2, **TRPC6**

Calcineurin components:

   PPP3CA, **PPP3CB**, **PPP3R1**

Downstream effectors:

   NFATC3, NFAT5, CAMK2D, CAMK4, CAMKK2

Others (associated with calcium signaling):

   RAP1B, RAP2B, MYH10, MYH11, HDAC9, MYH11, HDAC5, MEF2D, TPM4, ACTC1, PRKAR1A

Supplemental Table S3. The positions of TRPC6, PPP3CA, PPP3CB, PPP3R1, and NFATC3 in the ranking of transcript abundance based on human glomerular microarray profiling of ~20,000 genes with detectable mRNA levels

	Genes	Abundance ranking among ~ 20,000 genes
Podocyte enriched genes	GAPDH	73
	NPHS1	128
	WT1	1032
	SYNPO	9249
TRPC family	TRPC1	3774
	TRPC2	15201
	TPRC3	14635
	TRPC4	9462
	TRPC5	19479
	TPRC6	4697
PPP3C family	PPP3CA	2246
	PPP3CB	1588
	PPP3CC	12726
PPP3R family	PPP3R1	5011
	PPP3R2	19119
NFAT family	NFATC1	15060
	NFATC2	11824
	NFATC3	3984
	NFATC4	13112

Supplemental Table S4. The sequences of the primers used in the study.

Primer Name	Primer Sequence 5`-3`	Primer Name	Primer Sequence 5`-3`
H-PPP3CA-F	GCGCATCTTATGAAGGAGGGA	M-Ppp3ca-F	GTGAAAGCCGTTCCATTTCCA
H-PPP3CA-R	TGACTGGCGCATCAATATCCA	M-Ppp3ca-R	GAATCGAAGCACCCTCTGTTATT
H-PPP3CB-F	CCCCAACACATCGCTTGACAT	M-Ppp3cb-F	AAAGCGTGCTGACACTCAAG
H-PPP3CB-R	GGCAGCACCCTCATTGATAATTC	M-Ppp3cb-R	TGGAGAGAATCCTCGTATTGCT
H-PPP3CC-F	ACCGCGTCATCAAAGCTGT	M-Ppp3cc-F	ATGCCACCCCGAAAAGAGG
H-PPP3CC-R	CTTCCAGTCGTCCTTCCTTTAC	M-Ppp3cc-R	CATGGTCGGTCCTTCTTGACG
H-PPP3R1-F	CCTTTGGAAATGTGCTCACACT	M-Ppp3r1-F	ATGGGAAATGAGGCGAGTTACC
H-PPP3R1-R	GGATTCTGTTGTAACTCAGGCAG	M-Ppp3r1-R	TCCACGCTCAAAGAACCAGAA
H-PPP3R2-F	GCAGAAGTTGAGGTTTGCGTT	M-Ppp3r2-F	AAATGAGGCCAGCTACCAAAC
H-PPP3R2-R	TCTTGTGGATCTCCAGGTCTC	M-Ppp3r2-R	CCCGATTTGTCCAAGTCCAG
H-NFATC1-F	GCAGAGCACGGACAGCTATC	M-Nfatc1-F	GACCCGGAGTTCGACTTCG
H-NFATC1-R	GGGCTTTCTCCACGAAAATGA	M-Nfatc1-R	TGACACTAGGGGACACATAACTG
H-NFATC3-F	GCTCGACTTCAAACTCGTCTT	M-Nfatc3-F	GTATGGATCTGGACACTCCTTGT
H-NFATC3-R	GATGCACAATCATCTGGCTCA	M-Nfatc3-R	CGTCGTTTACCACAGGGAGA
H-NFATC2-F	GCTGGTTCCGGTGTACTCG	M-Nfatc2-F	CCACCACGAGCTATGAGAAGA
H-NFATC2-R	AGAGACCACTCGAATCTGCCA	M-Nfatc2-R	GTCAGCGTTTCGGAGCTTCA
H-NFATC4-F	CTTCTCCGATGCCTCTGACG	M-Nfatc4-F	GAGCTGGAATTTAAGCTGGTGT
H-NFATC4-R	CGGGGCTTGGACCATACAG	M-Nfatc4-R	CATGGAGGGGTATCCTCTGAG
H-TRPC1-F	AGGAACTAGCCCGGCAATGTA	M-Trpc1-F	TACGGTTGTCAGTCCGCAGA
H-TRPC1-R	GCTCGTCACTAGACGTATGGTTT	M-Trpc1-R	TCGTTTTGGCCGATGATTAAGTA
H-TRPC2-F	AACATCCTGCCCTCCTCGAAG	M-Trpc2-F	CTCAAGGGTATGTTGAAGCAGT
H-TRPC2-R	AGCAACAGCAAATGAACTGGCAA	M-Trpc2-R	GTTGTTTGGGCTTACCACACT
H-TRPC3-F	AGCAGCTCTTGACGATCTGG	M-Trpc3-F	TCGAGAGGCCACACGACTA
H-TRPC3-R	GCACAACGAGACACTTGATAGC	M-Trpc3-R	CTGGACAGCGACAAGTATGC
H-TRPC4-F	CGGCCTGGTAACATTCTGCT	M-Trpc4-F	TCCCACTGAGGATTGTCAGAG

H-TRPC4-R	GTTTGTCCCTCTCCGTCAAAAA	M-Trpc4-R	TCTTGACGCTTGCATAGTCCC
H-TRPC5-F	CTCTCGCTCCCGACTGAAC	M-Trpc5-F	AGCCCAGCATAAGCGACAAC
H-TRPC5-R	GAAGGCAGTTAGGATGGGGTC	M-Trpc5-R	GGCCTGAACCCATACTTACTCTG
H-TRPC6-F	CGGCTACTACCCCTGCTTC	M-Trpc6-F	AGCCAGGACTATTTGCTGATGG
H-TRPC6-R	CTTGTGGAGCGATCACTAAACA	M-Trpc6-R	AACCTTCTTCCCTTCTCACGA
H-NPHS1-F	CTGCCTGAAAACCTGACGGT	M-Nphs1-F	TCAAATGCACAGCCACCAAT
H-NPHS1-R	GACCTGGCACTCATACTCCG	M-Nphs1-R	TGCTGACGAGCTGGATGTTG
H-NPHS2-F	ACCAAATCCTCCGGCTTAGG	M-Nphs2-F	AGTGGAGAGAACTGAAATTAAGGATGT
H-NPHS2-R	CAACCTTTACGCAGAACCAGA	M-Nphs2-R	CCGCCAGAGAGTGCTGAAG
H-WT1-F	CACAGCACAGGGTACGAGAG	M-Wt1-F	CGGCGGAGTGCTTAGATGAG
H-WT1-R	CAAGAGTCGGGGCTACTCCA	M-Wt1-R	CTCGCTTCCGTTCCTTCTGT
H-SYNPO-F	ATGGAGGGGTACTCAGAGGAG	M-Synpo-F	GGCAGAGGGTGAACGAGTTC
H-SYNPO-R	CTCTCGGTTTTGGGACAGGTG	M-Synpo-R	GGGCCTCTTGGTTGAGCTTT
H-SMAD3-F	TGGACGCAGGTTCTCCAAAC	M-Smad3-F	CACGCAGAACGTGAACACC
H-SMAD3-R	CCGGCTCGCAGTAGGTAAC	M-Smad3-R	GGCAGTAGATAACGTGAGGGA
H-VHL-F	GGAGCCTAGTCAAGCCTGAGA	M-Vhl-F	TGTGCCATCCCTCAATGTCG
H-VHL-R	CATCCGTTGATGTGCAATGCG	M-Vhl-R	GCACCGCTCTTTCAGGGTA
H-ITGB4-F	CTCCACCGAGTCAGCCTTC	M-Itgb4-F	GCAGACGAAGTTCCGACAG
H-ITGB4-R	CGGGTAGTCCTGTGTCCTGTA	M-Itgb4-R	GGCCACCTTCAGTTCATGGA
H-B-ACTIN F	GCAAGCAGGAGTATGACGAGT	M-B-Actin F	ACCGTGAAAAGATGACCCAG
H-B-ACTIN	CTGCGCAAGTTAGGTTTTGTC	M-B-Actin R	AGCCTGGATGGCTACGTACA
R-Trpc6-F	AGCCAGGACTATTTGCTGATGG		
R-Trpc6-R	AACCTTCTTCCCTTCTCACGA		
R-Ppp3ca-F	GTGAAAGCCGTTCCATTTCCA		
R-Ppp3ca-R	GAATCGAAGCACCCTCTGTTATT		
R-Ppp3cb-F	AAAGCGTGCTGACACTCAAG		

R-Ppp3cb-R	TGGAGAGAATCCTCGTATTGCT
R-Ppp3r1-F	ATGGGAAATGAGGCGAGTTACC
R-Ppp3r1-R	TCCACGCTCAAAGAACCAGAA
R-Nfatc3-F	GTATGGATCTGGACACTCCTTGT
R-Nfatc3-R	CGTCGTTTACCACAGGGAGA
R-B-Actin-F	ACCGTGAAAAGATGACCCAG
R-B-Actin-R	AGCCTGGATGGCTACGTACA

References

1. Woroniecka, K.I., Park, A.S., Mohtat, D., Thomas, D.B., Pullman, J.M., and Susztak, K. 2011. Transcriptome analysis of human diabetic kidney disease. *Diabetes* 60:2354-2369.